Multiple Inequivalent Metal−Nucleotide Coordination Environments in the Presence of the VO^{2+}-Inhibited Nitrogenase Iron Protein: pH-Dependent Structural Rearrangements at the Nucleotide Binding Site†

Jan Petersen,* Karl Fisher,‡ Claire J. Mitchell,§ and David J. Lowe

Department of Biological Chemistry, John Innes Centre, Colney Lane, Norwich NR4 7UH, U.K.

Received April 22, 2002; Revised Manuscript Received August 5, 2002

ABSTRACT: Nitrogenase naturally requires adenosine nucleoside triphosphates and divalent metal cations for catalytic activity. Their energy of hydrolysis controls several mechanistic functions, most probably via separate structural conformers of the nitrogenase Fe protein. To characterize the ligand environment of the divalent metal in the ternary complex, with ADP or ATP and the Fe protein from *Klebsiella pneumoniae*, the hyperfine structures have been investigated by electron paramagnetic resonance (EPR) spectroscopy by substituting naturally occurring diamagnetic Mg^{2+} by paramagnetic oxovanadium. This metal replacement leads to inhibition of nitrogenase activity. Moreover, depending on pH, two distinctly different VO^{2+} EPR spectra are detected. At pH 7.4 each of the vanadyl EPR hyperfine lines is further split into two. This indicates that several spectroscopically distinguishable metal coordination environments coexist for VO^{2+}−nucleotide chelate complexes in the presence of the reduced Fe protein. Overall, a total of at least three distinct local metal coordination environments have been identified. We report the EPR parameters for each of the disparate metal coordinations measured at different pH values with ADP and ATP bound. EPR spectra have also been recorded for the oxidized Fe protein showing essentially similar spectra to that of the reduced protein. The EPR parameters of VO−nucleotides in the presence of the Fe protein are consistent, for all metal coordination environments, with direct metal ligation by nucleotide phosphate groups and the formation of mononucleotide complexes. The nucleotide binding environment with the highest ligand field strength is compatible with a metal coordination structure that is also found in various G-proteins with GTP bound. No significant EPR line width change is detected after exchange into D_2O buffer solution for any of the pH forms although differences exist between the pH forms. The missing difference between the EPR parameters in the presence of ADP or ATP suggests that there is little or no conformational rearrangement between these two forms; this contrasts with behavior of G-proteins that undergo substantial conformational changes upon hydrolysis. This could be related to the inhibition of nitrogenase by VO^{2+}.

The nitrogenase iron protein is encoded by the *nifH* gene and is one of two protein components that comprises the minimal functional unit required by diazotrophic organisms for enzymatic reduction of dinitrogen to ammonia (see, e.g., refs *1* and *2*) according to the reaction:

$$N_2 + 8H^+ + 16M^{2+}ATP + 8e^- \rightarrow 2NH_3 + H_2 + 16M^{2+}ADP + 16P_i \quad (1)$$

The reaction requires eight electrons, which are critical for the stepwise reduction of dinitrogen on the second nitrogenase component protein, the $\alpha_2\beta_2$ heterotetrameric MoFe protein. According to reaction 1, for each electron released for interprotein electron transfer from the Fe protein to the MoFe protein, a minimum of two ATP[1] molecules are hydrolyzed to ADP and inorganic phosphate (*2*). Nucleotide binding and hydrolysis occur on the nitrogenase Fe protein (*3*) while substrate reduction takes place on the MoFe protein. The Fe protein (M_r ~60000) consists of two identical subunits (γ_2-dimer structure) and contains a [4Fe-4S] cluster that yields a rhombic EPR signal when the Fe protein is reduced and is EPR silent when it is oxidized. Divalent metal ions M^{2+}, usually Mg^{2+}, are absolutely required in order for nucleotides to bind to the Fe protein (*4*) where ATP is an essential cofactor for substrate reduction whereas ADP is a competitive inhibitor. Mg^{2+} di- and triphosphate nucleosides bind tightly to the Fe protein in a positive cooperative manner

† This work was supported by a DTI LINK grant with BBSRC, Zeneca Agrochemicals, and Bruker Spectrospin. D.J.L. thanks BBSRC for financial support through the Core Strategic Grant to the John Innes Centre.

* Address correspondence to this author. Fax: 44-1603-450018. E-mail: jan.petersen@bbsrc.ac.uk.

‡ Present address: Department of Biochemistry, Virginia Polytechnic Institute and State University, Blacksburg, VA 24061.

§ Present address: Ballinrobe Community School, Ballinrobe, Co. Mayo, Eire.

[1] Abbreviations: EPR, electron paramagnetic resonance; ENDOR, electron nuclear double resonance; ESEEM, electron spin−echo envelope modulation; Av2, Cp2, and Kp2, nitrogenase iron protein from *Azotobacter vinelandii*, *Clostridium pasteurianum*, and *Klebsiella pneumoniae*, respectively; ADP (GDP), adenosine (guanosine) 5′-diphosphate; ATP (GTP), adenosine (guanosine) 5′-triphosphate; Tris, tris(hydroxymethyl)aminomethane; hf(c), hyperfine (coupling).

10.1021/bi0260029 CCC: $22.00
Published on Web 10/11/2002

(*2*), with MgADP binding more tightly than MgATP. However, reported dissociation constants vary depending on factors including the method of measurement, the specific activity of the protein, and the organism employed (*1*). Differences between the reduced and oxidized states of the protein have also been observed (*5*, *6*).

The X-ray crystal structures of several nitrogenase Fe protein preparations have now been analyzed as well as the nitrogenase heteroprotein complex consisting of the Fe and MoFe protein. Structures of the isolated Fe protein contained either no cosubstrate Mg^{2+}−nucleotide complex at all (*7*), ADP and two molybdate ions without bound Mg^{2+} (*8*), or two ADP and Mg^{2+} ions (*9*). The first study of the Fe protein from *Azotobacter vinelandii* (*8*) revealed that the [4Fe-4S] cluster is located at the interface of the two protein subunits, at a sort of pivotal point between them. In addition, the protein contained substoichiometric amounts of, presumably, very tightly bound ADP. This nucleotide bridges the subunits, with the adenosine moiety in contact with one subunit and the phosphate groups contacting the other, at a distance of about 20 Å from the cluster center. In the crystal structure two molybdate ions were present, one on each subunit, probably occupying the γ-phosphate position of the ATP site. It is notable that substantially less than one nucleotide per subunit copurified and no Mg^{2+} was bound. More recently, the X-ray crystal structure of Av2 in the presence of MgADP has also been determined (*9*). Moreover, two nitrogenase complexes have been analyzed: the Av1−Av2 complex structures with Mg^{2+}, ADP, and AlF_4^- bound (*10*) and a catalytically inactive altered protein structure with Mg^{2+} and ATP bound (*11*). Both complexes possess two nucleotides bound per Fe protein, or four per nitrogenase complex. The native Fe protein has not yet been crystallized with ATP or a nonhydrolyzable ATP analogue. Even though significant progress has been made and the crystal structure of the Fe protein is now known, the exact hydrolysis mechanism and its regulatory function still remain largely uncharacterized. Numerous questions are left unanswered including whether the observed nucleotide binding site on the Fe protein is the only site where hydrolysis occurs, how information about the presence of nucleotides is transmitted to the cluster 20 Å away, the exact functional role of the nucleotides and the mechanism by which ATP is hydrolyzed, and how hydrolysis relates to electron transfer and what exactly triggers the component proteins to dissociate after electron transfer.

Several lines of evidence suggest that binding and hydrolysis of nucleotides are accompanied by significant structural rearrangements within the Fe protein; in particular, a change occurs to a more axial [4Fe-4S] cluster EPR signal (*12*, *13*). A continuum of protein conformational changes is actually believed to modulate the complex functions of nitrogenase, such as electron transfer and protein association/dissociation coupled to MgATP binding, P_i hydrolysis, P_i release into solution, and repositioning of Mg^{2+}, finally ending in the coproduct (MgADP) bound state (*9*). Apart from the X-ray structures these conformational changes have generally only been detected spectroscopically indirectly by observing a distinct change at the FeS cluster. The X-ray crystal structure of the Fe protein−MoFe protein complex has graphically established the conformational changes upon aggregation, but it does not yield information on alterations happening on nucleotide hydrolysis, or change of oxidation state, which are presumably responsible for complex dissociation. A detailed analysis of the coordination environment of the metal center bound to ADP or ATP and of the reduced and oxidized Fe protein might assist in elucidating the complex metal−nucleotide coordination environments in the various forms.

Because the divalent metal binding site is likely to be intimately associated with the signal transduction mechanism (*9*, *14*), in this work we have investigated the protein conformation directly at the nucleotide binding site by using the metal center bound to the nucleotide, i.e., vanadyl, as the spin probe. Vanadium(IV), as oxovanadium with a net charge of +2 is EPR active and was used here for substitution of the usual diamagnetic Mg^{2+} ion. The vanadyl ion $(V^{IV}{=}O)^{2+}$ has a $3d^2$ ground state, and perturbation by the oxygen atom lifts the otherwise 3-fold t_{2g} degeneracy to give a ground state $S = {}^1/_2$ Kramer's doublet from which the higher energy levels are energetically well separated. The unpaired electron resides predominantly in a nonbonding d_{xy} orbital (*15*). The hyperfine structure of the VO^{2+} ion gives eight resolved EPR lines, due to the coupling to the ^{51}V ($I = {}^7/_2$) nuclear spin, which are further split in polycrystalline spectra into "powder-type" parallel and perpendicular resonances due to *g*-value and hyperfine anisotropy. In the present study we report the metal hyperfine interactions obtained by EPR that allow us to characterize the coordination environment of VO−ADP and VO−ATP in the presence of the Fe protein and demonstrate that with VO^{2+} (replacing Mg^{2+}) major conformational rearrangements at the metal binding site can be observed. These studies provide information obtained from a spin probe bound directly at the site of ATP hydrolysis and on rearrangements implicated to be essential factors modulating the complex electron-transfer reactions in the Fe protein (*16*). We further demonstrate that conformational rearrangements of the Fe protein not only occur upon nucleotide hydrolysis but also as a function of pH.

MATERIALS AND METHODS

Sample Preparation. The Fe protein of the bacterial diazotroph *Klebsiella pneumoniae* NCIB 12204 (Kp2) was purified under strictly anaerobic conditions and characterized as reported by Thorneley and Lowe (*17*). All experiments with the nitrogenase Fe protein in the presence of VO−nucleotides were carried out in a 50 mM Tris buffer solution after the protein was exchanged into Mg-free buffer by gel filtration. The final solutions contained 250 mM NaCl instead of the 90 mM $MgCl_2$ normally used. The metal−nucleotide was added from pH adjusted, premixed stock solutions with a 9-fold excess of adenosine 5′-diphosphate or adenosine 5′-triphosphate nucleotides over $VOCl_2$. Solutions of the reduced Fe protein contained 5 mM sodium dithionite unless otherwise stated. Protein concentrations, after purification and subsequent concentration using Minicon B-15 macrosolute concentrators (Amicon), were 150−170 mg/mL. All operations were conducted in an anaerobic glovebox. Anaerobic conditions also prevent aerobic oxidation of VO^{2+} to VO_2^+ (*18*).

Preparations exchanged into D_2O buffer were treated, using a similar procedure to that for removal of Mg^{2+}, by running purified protein down a Bio-Gel P-6DG column (Bio-Rad, Watford, Herts, U.K.) equilibrated with D_2O (99.9% isotopic

purity). $VOCl_2$ was added to nucleotide before addition to the protein. To exclude the possibility that the water exchanges extremely slowly with D_2O, we also performed experiments for preparations which were incubated with D_2O over several hours and observed no further change of the EPR line width.

Oxidation of Kp2 protein was achieved using the dye indigo carmine (AnalaR grade) as described by Ashby and Thorneley (*6*) with the exception that a much larger Bio-Gel P-6DG column (1.5 cm × 20 cm) was used. The protein was concentrated using Minicon B-15 concentrators after elution from the column to increase the concentration to the desired level.

Activity Assay. The specific activity in the presence of oxovanadium nucleotides was assayed by monitoring the reduction of acetylene to ethylene as described elsewhere (*17*). Assays were carried out at low salt concentrations (NaCl <30 mM). The specific activity in the presence of 12.5 mM $VOCl_2$ and 5 mM ATP was less than 1% of that with 12.5 mM $MgCl_2$ and 5 mM ATP. Competition experiments were performed at pH 7.5 and 30 °C using a Kp2:Kp1 molar ratio of 4:1 plus 9 mM ATP and 12.5 mM $MgCl_2$ by monitoring C_2H_4 production as a function of $VOCl_2$ concentration. The $VOCl_2$ concentration was varied from 0 to 12.5 mM and showed an essentially linear decrease of the specific activity, from ca. 1300 nmol of C_2H_4 (min·mg of Fe protein)$^{-1}$ at zero $VOCl_2$ to less than 20 nmol of C_2H_4 (min·mg of Fe protein)$^{-1}$ above 10 mM $VOCl_2$. Thus replacing Mg^{2+} by VO^{2+} has the additional advantage, besides its favorable spectroscopic properties, that no non-hydrolyzable ATP analogue needs to be used.

EPR Spectroscopy. Low-temperature X-band EPR spectra were recorded on a standard Bruker ESP300 spectrometer slightly modified to accommodate quartz EPR sample tubes up to 5 mm o.d. The spectrometer was fitted with a conventional liquid helium Oxford Instruments ESR900 flow cryostat for which the sample temperature had been calibrated with a thermocouple at the sample position inside the quartz dewar. The temperature was controlled by an Oxford Instruments ITC4 temperature controller. The values for the occupancy of particular conformations have been determined from the peak intensities of the EPR transition, not from integrations. The spin Hamiltonian parameters have been calculated by individual spectral simulation of the composite EPR spectra using the program LSIM. The experimental EPR line width was determined as the width at half-height.

RESULTS

The X-ray crystal structure of one of the two almost identical metal−nucleotide binding sites of homodimeric Av2 in the ADP-bound or "off" conformational state in the presence of the naturally coordinated divalent Mg^{2+} ion (*9*) is shown in Figure 1. The 6-coordinate metal is bound in a monodentate, "head-on" configuration to one of the phosphate oxygens of ADP. The only direct protein contact is via a serine side-chain O_δ interaction. The other four ligand positions are occupied by water which in at least two cases forms bridges to protein carboxyl side chains. This structure closely resembles the Mg−diphosphate nucleotide binding site composition of other nucleotide binding proteins as discussed below. The inner-sphere metal coordination geometry is best described as square bipyramidal, with two water molecules coordinated in the equatorial plane.

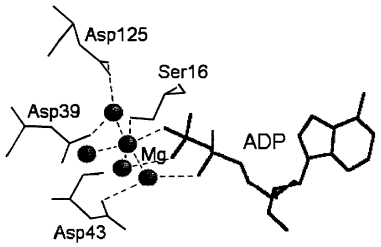

FIGURE 1: X-ray crystal structure of the metal−nucleotide coordination environment of the ternary complex consisting of the nitrogenase Fe protein from *A. vinelandii*, Mg^{2+}, and ADP (PDB coordinates: ID code 1FP6).

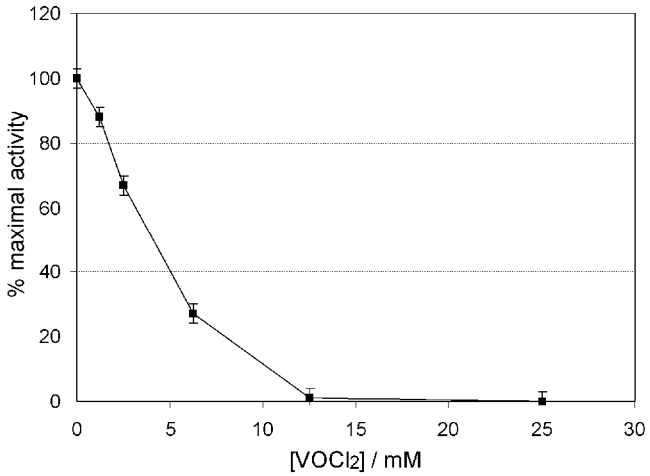

FIGURE 2: Nitrogenase specific activity in the presence of vanadyl relative to maximal activity obtained in the absence of $VOCl_2$. The competition experiment has been carried out in the presence of 12.5 mM $MgCl_2$ at a Kp2:Kp1 molar ratio of 4:1.

The effect of vanadyl concentration on nitrogenase activity has been probed by using protein activated with Mg^{2+}. The inhibition of ethylene production by nitrogenase through the addition of VO^{2+} is depicted in Figure 2, showing the ability of VO^{2+} to compete effectively with Mg^{2+} for nucleotide binding.

The frozen solution X-band EPR spectra of oxovanadium, at two different pH values, in the presence of ATP and reduced Fe protein of nitrogenase isolated from *K. pneumoniae* are shown in Figure 3. The spectra are superpositions of the signal from the VO^{2+} complex and the $S = {}^1/_2$ signal of the $[4Fe\text{-}4S]^{1+}$ cluster from the dithionite-reduced Fe protein (*12*). The principal axis *g*-tensor components of the intrinsic cluster, measured in the absence of VO−nucleotides, are indicated by arrows in the figure. The vanadyl EPR spectrum is split by the hf interaction with the $I = {}^7/_2$ nuclear spin of ^{51}V into $(2I + 1)$ EPR lines. The top trace in Figure 3A shows the experimental spectrum for the sample at pH 6.4 and resembles the typical eight-line hyperfine-split vanadyl spectrum in a polycrystalline matrix found for other VO^{2+} complexes (*19*) with an almost axial **g** and hf tensor. At pH 7.4 the corresponding VO^{2+} spectrum is considerably different from that at the lower pH (Figure 3B, top trace). Thus, two substantially different vanadyl EPR spectra are detected, characteristic of low and neutral pH forms. Virtually identical pH dependencies were observed for spectra of VO−ATP and VO−ADP in the presence of reduced Kp2.

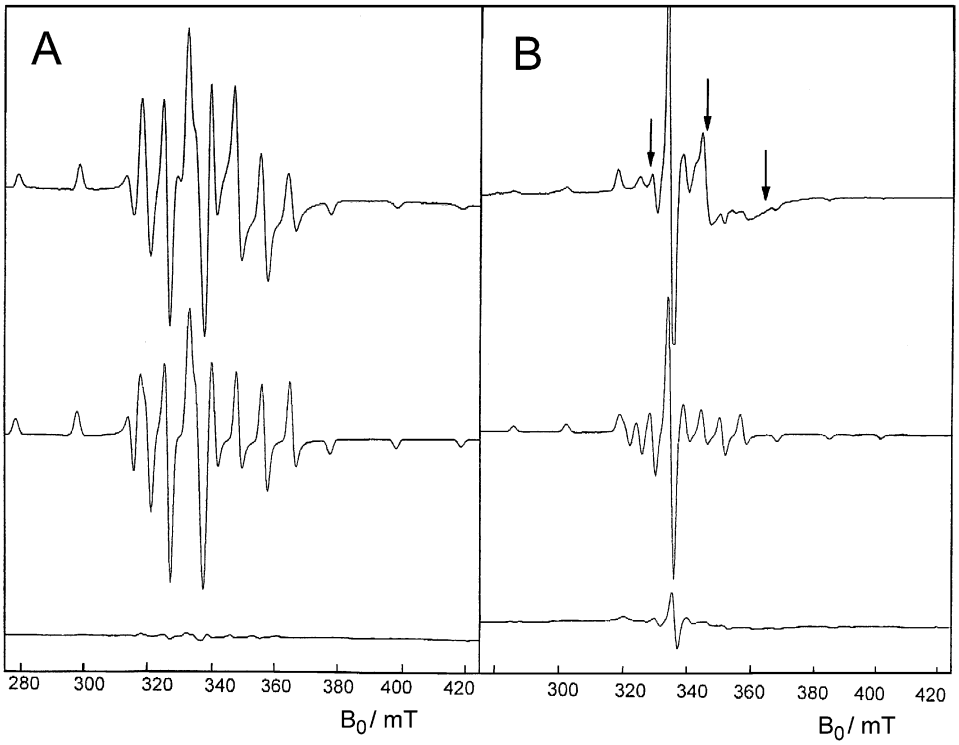

FIGURE 3: Frozen aqueous solution X-band EPR spectra of VO−ATP in the presence of reduced nitrogenase Fe protein from *K. pneumoniae* at different pH values. Buffer solutions contained 250 mM NaCl and 5 mM $Na_2S_2O_4$. The protein concentrations were approximately 140 mg/mL, and concentrations of $VOCl_2$ and ATP were 1 and 9 mM, respectively. The top spectra in (A) and (B) are the experimental spectra of the preparation at pH 6.4 and at pH 7.4, respectively. The middle spectra are the corresponding powder spectra simulations with the EPR parameters given in the text. Arrows indicate the principal axis *g*-value components of the FeS cluster of Kp2. The bottom traces in (A) and (B) are the spectra in the absence of protein and nucleotides. Experimental conditions: temperature, 20 K; microwave frequency, 9.44 GHz; microwave power, 0.2 mW; modulation frequency, 100 kHz; modulation amplitude, 1.58 mT.

The parameters used for the spectral simulations of a $S = {}^1/_2$ electron spin system from the $^{51}V(IV)$ ion in a randomly oriented rigid matrix coupled to an $I = {}^7/_2$ nuclear spin (middle traces in Figure 3A and 3B) demonstrate that significant differences exist between the local metal coordination environments for the two pH forms. The EPR parameters for the low and neutral pH forms indicate low and high ligand field strengths, respectively.[2] The bottom traces in Figure 3 are the spectra of VO^{2+} free in solution in the absence of protein and nucleotides. At these pH values, VO^{2+} free in solution precipitated, forming polymeric, EPR-silent $[VO(OH)_2]_n$ complexes (*19*). As these traces demonstrate, only negligible amounts (<15% at pH 7.4 and even less at pH 6.4) of VO^{2+} are detectable by EPR so that no significant amounts of VO^{2+}−Tris chelates form under our conditions in the absence of nucleotides and Kp2. Preparations containing reduced Kp2 and VO−ATP, instead of VO−ADP, give essentially identical spectra (data not shown), with the same resonance positions and intensity ratios.

Close inspection of the spectra reveals that each of the EPR hyperfine lines of samples at neutral pH is split into two components; this is most apparent for preparations in D_2O buffer and for EPR lines corresponding to an orientation of the magnetic field vector aligned along the V=O axis, i.e., the high-field parallel hf lines. A portion of the high-field region of the VO^{2+} EPR spectrum with the three $M_I = +3/2, +5/2$, and $+7/2$ parallel transitions is shown in Figure 4 on an expanded scale. Trace A represents the VO^{2+} spectrum for the VO−ADP complex with dithionite-reduced Kp2 in D_2O buffer (pD 7.4). The different line positions of the signal components arise from two inequivalent, superimposed, EPR spectra with different **g**- and **A**-tensor anisotropies with the high-field component being more intense.

As mentioned for the wide scan spectra (Figure 3), spectral comparisons of the $M_I = +{}^3/_2, +{}^5/_2$, and $+{}^7/_2$ parallel high-field transitions with VO−ATP bound to reduced Kp2 (data not shown) yield essentially similar resonance positions to those with VO−ADP in H_2O and D_2O buffer, and at about neutral pH(pD), with resonances from separate subspectra, whereas at low pH (pD), each of the hf lines only shows a single resonance. The similarity of the subspectra compositions suggests that the coordination environments of the metal centers are remarkably similar for both nucleotides.

The oxidized Fe protein binds nucleotides even more tightly than the reduced Fe protein (*2*). Figure 4 (trace C) illustrates the effect of the oxidation of Kp2 on the site specificity for the VO−ADP−Kp2 complex in D_2O buffer (pD 7.4). Again, each of the hf lines is split, with essentially identical resonance field values to those of the reduced Fe protein. However, oxidation of the Fe protein increases the proportion of the high-field component (only about 15% of the intensity remains in the low-field line compared to 35%

[2] Almost all VO^{2+} spectra in the presence of Kp2 can be explained within a system of axial or pseudoaxial symmetry without any significant rhombic distortion within our resolution. The deviation between the experimental spectrum and the simulation, which is most pronounced for the high-field side of the neutral pH spectrum is caused by the underlying $S = {}^1/_2$ FeS cluster signal, which was not included in the simulation.

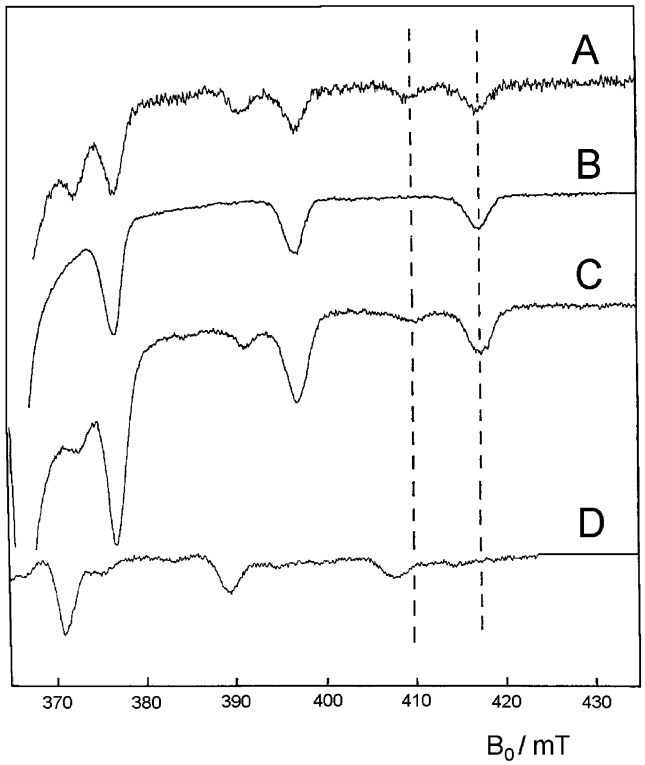

FIGURE 4: Comparison of the high-field portions of the EPR spectra of the VO−ADP complex in the presence of the Fe protein shown on an expanded scale with the $M_I = +3/2$, $+5/2$, and $+7/2$ parallel EPR lines indicated. Spectra are for (A) the dithionite-reduced Fe protein exchanged into D_2O buffer, pD 7.0, (B) the dithionite-reduced Fe protein at pH 5.0 and in H_2O containing buffer, (C) the indigo carmine-oxidized Fe protein at pD 7.0 in D_2O buffer, and (D) the VO−ATP complex prepared under identical conditions at pD 7.6 in D_2O buffer in the absence of protein. Spectra are averages of five scans recorded at a temperature of 20 K (A and C), 10 K (B), and 25 K (D). Other conditions were the same as for Figure 3.

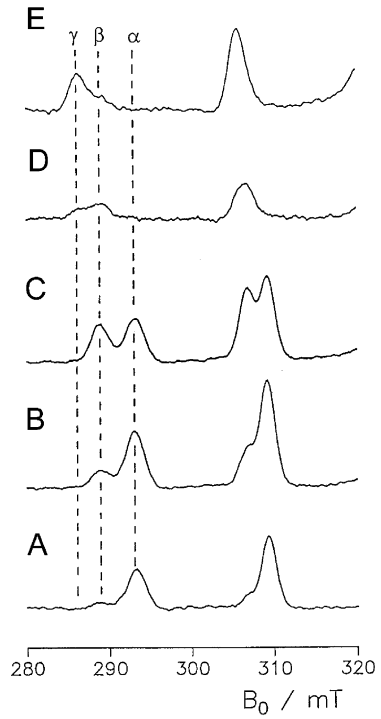

FIGURE 5: Frozen solution EPR spectra of VO^{2+}−ATP in the presence of reduced Kp2 in H_2O buffer solution at pH 7.5 for various concentration ratios of metal to protein. Spectra of the low-field region with the $M_I = -7/2$ and $M_I = -5/2$ parallel hf lines for a ratio of metal:Kp2 of 0.5:1 (A), 1:1 (B), 1.5:1 (C), 3:1 (D), and 5:1 (E) using 9 mM ATP. VO^{2+} spectral components are indicated for the $-7/2$ parallel hf line by the dashed lines and are labeled α, β, and γ. Experimental conditions: temperature, 25 K; microwave frequency, 9.63 GHz; microwave power, 0.2 mW; modulation frequency, 100 kHz; modulation amplitude, 0.24 mT.

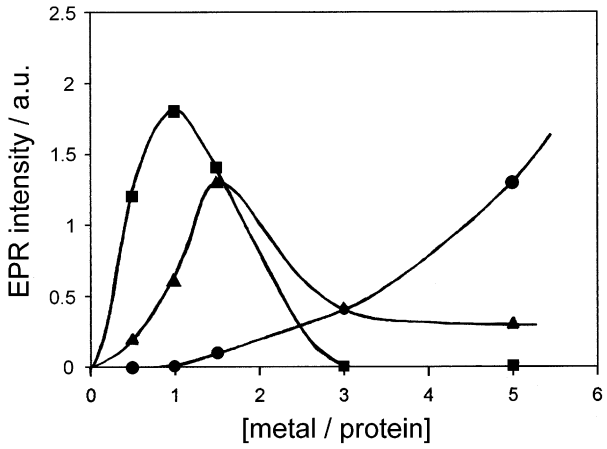

FIGURE 6: EPR intensities from the $M_I = -7/2$ parallel hf line of the three identifiable coordination environments as a function of the metal:protein concentration ratio. The pH is kept invariable at pH 7.5. Squares are for the α-conformation, triangles for the β-conformation, and circles for the γ-conformation.

with reduced Fe protein). Thus, the relative proportions of the two signal components appear to depend on the oxidation level of the Fe protein.[3]

Titration of Kp2 with increasing VO^{2+} concentration again shows that at least three distinguishable EPR subspectra can be identified, denoted α, β, and γ. They are seen most clearly for parallel hf lines and are indicated for the $M_I = -7/2$ parallel resonance for the three inequivalent metal environments by the dashed lines in Figure 5. It is apparent that the subspectrum with the hf line at the high-field side of the $-7/2$ parallel transition (α-conformation) is best discerned at low metal concentrations and clearly dominates at concentrations lower than 1:1 metal:protein ratios, while the subspectrum with resonances at the low-field side (γ-conformation) is only observed at high metal concentrations >2 VO^{2+}/Fe protein. The latter conformation has the largest parallel hf component, $A^{\|}$, corresponding to low ligand field strength, while the α subspectrum with the inner lines (smallest $A^{\|}$ component) has the highest ligand field strength. The third subspectrum (β-conformation) is most intense at intermediate metal concentrations. The regions where the various conformations yield maximal EPR intensities are most evident in Figure 6, which shows the EPR intensities as a function of the concentration ratio. The spectrum of the γ-conformation observed at neutral pH and high vanadyl concentrations is essentially identical to that for the low-pH form.

The spectra of Figures 4 and 5 also demonstrate that no additional superhyperfine structure, such as would be given by a strong ^{31}P coupling to a coordinating phosphate group,

[3] Note that the intensity distribution is also affected by the magnitude of the hyperfine coupling A, where the relative intensities of parallel hf lines for larger $A^{\|}$ values are generally less intense than those for smaller. This is most pronounced for the outer parallel hf lines and obstructs a direct comparison of intensities.

Table 1: EPR Spin Hamiltonian Parameters of VO^{2+} in the Presence of Nucleotides and the Dithionite-Reduced Nitrogenase Fe Protein from *K. pneumoniae*[a]

complex	conformation	$g^{\|\|}$	$g^{\perp}$	$A^{\|\|}/\times 10^{-4}$	$A^{\perp}/\times 10^{-4}$
VO(ATP)−$Kp2^{red}$ (pH 7.4)	α (β_2?)	1.942	1.993[b]	158.0	50.3[b]
	β (β_1?)	1.952	1.993[b]	165.7	50.3[b]
VO(ATP)−$Kp2^{red}$ (pH 6.4)	γ	1.937	1.987	178.7	66.5
VO(ADP)−$Kp2^{red}$ (pH 5)	γ	1.932	1.982	179.8	68.1
VO(ATP)−$Kp2^{red}$ in D_2O (pD 7.8)	α	1.963	1.987, 1.982[c]	151.6	43.9, 51.7[c]
	β	1.942	1.982	167.3	62.2
VO(ADP)−$Kp2^{red}$ in D_2O (pD 7.0)	β	1.945	1.983[b]	168.1	66.2[b]
	γ	1.932	1.983[b]	178.5	66.2[b]
VO(ATP)−$Kp2^{red}$ in D_2O (pD 6.0)	γ	1.937	1.986	179.1	66.5
VO(ADP)−$Kp2^{red}$ in D_2O (pD 6.5)	γ	1.941	1.985	179.6	67.3
VO(ADP)−$Kp2^{ox}$ in D_2O (pD 7.0)	β	1.945	1.981[b]	168.1	66.5[b]
	γ	1.932	1.981[b]	178.5	66.5[b]
VO(ATP) in D_2O (pD 7.6)	A_x	1.946	nd[d]	164.5	nd

[a] Determined by the method of Chasteen (*19*) (see text for details). The values for the principal axis hyperfine coupling components, $A^{\|\|}$ and $A^{\perp}$, are in cm^{-1}. [b] Differences between the parameters for the two conformations cannot be determined due to insufficient discrimination of the subspectra. [c] Separate parameters are most likely caused by a rhombic distortion. [d] nd: not determined.

is resolved for any of the EPR hf lines. A similar observation was made even after exchange into D_2O buffer solution (data not shown). This was not the case for any of the VO^{2+} hf lines or for preparations at low and neutral pH. However, a strong shf coupling to phosphorus nuclei has been detected by ENDOR spectroscopy (*32*).

Multiple inequivalent pH-dependent VO^{2+}−nucleotide coordination environments have been identified in the presence of Kp2. All spin Hamiltonian parameters determined for various preparations at different pH values with VO−ADP and VO−ATP in the presence of Kp2 are listed in Table 1. The data suggest that the β-conformation might be further composed of two distinctly separate coordination environments with slightly different spin Hamiltonian parameters as discussed below. The subspectrum with the smallest hf parameters is given by the α-conformation with somewhat unusually low values of $A^{\|\|}$ and $A^{\perp}$ for VO^{2+} in biological environments. $A^{\|\|}$ values reported so far for VO^{2+} in proteins normally range between about $157-180 \times 10^{-4}$ cm^{-1} (*19*) with two exceptions, imidazole glycerol phosphate dehydratase (*20*) and F_1-ATPase (*21*). It should be noted that the latter is also the only other nucleotide binding protein that has been studied in detail in the presence of vanadyl ions. Intriguingly, the VO^{2+}−nucleotide binding structure of F_1-ATPase with ADP bound at one of the sites, reported to be that of the catalytic β_{TP} activated form, has an $A^{\|\|}$ value of 155×10^{-4} cm^{-1} that is remarkably close to one of the values we measure for the neutral pH form of Kp2.

Most of the EPR spectra for the VO−nucleotide−Fe protein complexes can be interpreted within a system of axial or pseudoaxial symmetry with no resolvable rhombic distortion. The only spectrum for which a slight rhombicity was identified is that for the VO−ATP complex with reduced Kp2 in D_2O buffer (pD 7.8) (cf. Table 1). It is, however, possible that the spectra of corresponding preparations with VO−ADP, or in H_2O buffer, exhibit a similar rhombic distortion for the perpendicular hf lines which is not resolved because it is masked by the convolution of subspectra and a slightly broader line width. The magnitude of the $A^{\perp}$ value suggests that the rhombic distortion occurs in the α-conformation. Nonetheless, it is obvious from the spectra that substantial spectral changes occur when going from the high- to the low-pH form, pertaining to a substantial change of **g** and **A** tensor, especially a decrease of the hf coupling components $A^{\|\|}$ and $A^{\perp}$. This large pH effect on the EPR parameters suggests that a substantial rearrangement in the inner-coordination environment of the metal center occurs as a function of pH.

EPR spectra for preparations in H_2O or D_2O buffer solution can both be simulated with virtually identical line width parameters, namely, $\Gamma = 1.7$ mT. The experimental line width determined for the $M_I = -5/2$ parallel hf line for preparations at low pH is about 1.8 mT independent of the used nucleotide or deuteration status of the solvent. On the other hand, when the pH is raised, the line width increased. A line width of about 2.5 mT was measured for preparations at about neutral pH and above. Thus the only significant differences are observed between the γ-conformation (dominating at low pH) and the α-conformation (dominating at neutral pH and low metal:protein ratio). This suggests that there are no or only few water molecules bound in the equatorial metal plane.[4]

DISCUSSION

Vanadium is known to be a potent inhibitor of a variety of proteins where it is usually bound as vanadate (see, e.g., ref *22*). Nonetheless, there is also a smaller number of proteins that are inhibited by vanadyl; these include ribonuclease (*23*), receptor tyrosine kinases (*24*), and imidazole glycerol phosphate dehydratase *(20)*. Here we have shown that VO^{2+} inhibits acetylene reduction by disrupting the ATPase activity at the Fe protein.

The presence of separate, spectroscopically distinguishable, vanadyl EPR spectra shows that VO^{2+}−nucleotides in the presence of Kp2 undergo a critical rearrangement in the inner-sphere metal coordination environment as a function of pH with at least three identifiable coordination environments, α, β, and γ, which partially coexist.[5] The EPR parameters of these coordination environments can yield valuable information about the ligand environment of the

[4] However, line width changes could be masked by couplings to other ligand nuclei, such as phosphorus groups.

[5] The general relationship $g_e > g^{\perp} > g^{\|\|}$ (*15*) is fulfilled for all three coordination environments and therefore indicates that the vanadyl metal center symmetry is C_{4v} in all three cases.

metal. The low-pH form found in the present study is that of a system of low ligand field strength, with the $A^{||}$ value relatively close but not identical to the value for the weak field limit of the pentaaquo−VO^{2+} complex with $A^{||} = 182.6 \times 10^{-4}$ cm^{-1} (*25*). The spin Hamiltonian parameters for the γ-conformation are essentially identical with those measured for VO^{2+}ATP complexes (pH 5.0) in the absence of protein with an $A^{||}$ value of 180.1×10^{-4} cm^{-1} (*26*). The high-pH forms observed at low to moderate VO^{2+} concentrations, on the other hand, have values for $A^{||}$ and $A^{\perp}$ which are relatively low and indicate a relatively strong ligand field. The simultaneous presence of separate, spectroscopically distinguishable, vanadyl EPR spectra in proteins indicates that different local metal center coordination environments exist. Their pronounced pH dependence is not unusual and has been previously observed for a number of proteins including carboxypeptidase A (*27*), apoferritin (*28*), chloroperoxidase (*29*), D-xylose isomerase (*30*), and imidazole glycerol phosphate dehydratase (*20*). Vanadyl nucleotides in the absence of protein, on the other hand, show only a single vanadyl coordination environment (*26*, *31*). Therefore, multiple coordination environments, observed here, are directly associated with the formation of the protein complex.

The correlation of the ligand field strength for the VO^{2+} ion, derived from the spin Hamiltonian EPR parameters, i.e., the $g^{||}$ and the $A^{||}$ values, can be used to give to some extent an indication of the nature of the equatorial ligands of the metal center (*19*). Using the sum formula of Chasteen (*19*):

$$A^{||}_{calc} = \sum_i n_i A^{||}_i / 4 \qquad (2)$$

where i sums over the different ligands and assuming that the contribution of one equatorial ligand is independent of the other three, one can calculate the parallel VO^{2+} hf component for different donor group composition.

γ-Conformation. The EPR parameters for the low-pH form suggest that the equatorial coordination environment contains some H_2O ligands, or ligands with $A^{||}_i$ values close to those for H_2O such as carboxylates. From a consideration of the nitrogenase X-ray crystal structures, a comparison with other "classical" nucleotide binding proteins (vide infra), and results from synthetic metal−nucleotide chelate complexes, it appears reasonable to assume that the metal possesses at least some inner-sphere phosphate oxygen ligands originating from coordination to the nucleotide phosphate chain. The most probable number of coordinated phosphate groups for the ATP complex is two. On the basis of this assumption and given the experimental EPR parameters for that particular site, we assume that, in addition to two phosphate oxygens with individual values of $A^{||}_i = 171 \times 10^{-4}$ cm^{-1} (*32*), two H_2O ligands comprise the equatorial inner-sphere coordination shell, yielding a calculated value of $A^{||}_{calc} = 176.8 \times 10^{-4}$ cm^{-1}. This is in reasonably good agreement with the experimental value of about 179×10^{-4} cm^{-1} and still within the acceptable error of 3×10^{-4} cm^{-1} laid down by Chasteen (*19*). This interpretation holds for both the VO−ADP and VO−ATP bound forms because the γ-conformation for these two yields very similar $A^{||}$ values (cf. Table 1), which implies that the number of coordinated phosphate groups is invariant for VO^{2+} with ADP or ATP. However, due to the similarity of $A^{||}_i$ values, especially for carboxyl and phosphate oxygen ligands but also for water ligands, this interpretation needs to be viewed with some caution.

Alternatively, a tridentate nucleoside coordination is conceivable for the γ-conformation such as observed for the bisnucleotide complex $[M(H{\cdot}ATP)_2]^{4-}$ with $M = Mg^{2+}$ or Ca^{2+} without any protein (*33*). However, this would result in an even lower $A^{||}_{calc}$ value of 173.9×10^{-4} cm^{-1}, and the interpretation of subsequent ^{31}P ENDOR (*34*) spectra opposes this consideration. VO^{2+} could also have only one nucleotide ligand. Such a coordination structure has been reported for the dissimilar nitrogenase complex of the LeuΔ altered Fe protein with MgATP (*11*) and for one of the binding sites (α_{DP}) with VO^{2+}−ATP in F_1-ATPase, with three equatorial waters, giving a value of $A^{||} = 181.5 \times 10^{-4}$ cm^{-1} (*21*). This value is again close to the spin Hamiltonian parameters of the γ-conformation and is consistent with the ADP-bound X-ray crystal structure (cf. Figure 1). However, we consider this interpretation less likely since no EPR line narrowing was observed on exchange of preparations in the low-pH form into D_2O buffer nor were ^{1}H ENDOR resonances found that were consistent with equatorial water coordination (*35*). This contrasts with the X-ray crystal structures of the Fe protein from *A. vinelandii* (*9*) and G-proteins, such as the MgGDP-bound p21Ras oncogene product (*36*, *37*), which all gave evidence for the presence of at least one equatorial water molecule in the inner-coordination shell of the ADP/GDP-bound conformation. This apparent discrepancy for the γ-conformation (and in part also for one of the β-conformations) is not yet fully understood.

It has been demonstrated that it is virtually impossible to distinguish between 5- and 6-coordinate vanadyl complexes purely on the basis of the EPR spin Hamiltonian parameters (*38*, *39*). Thus, in the present study, we cannot exclude that the VO^{2+} center is 5-coordinate, which could have one coordinated water less. ENDOR studies, however, are characteristic of hexacoordination (*35*). Furthermore, it has to be noted that the additivity relationship of Chasteen (*19*) has its limitations because, for example, it does not take into account the axial ligand, possible changes of the EPR parameter through multidentate coordination with mixed equatorial and axial ligation, or the relative orientation of the ligands within the equatorial plane (*40*). As a consequence of the probable water coordination (with two equatorial and one axial water ligand) we conclude that the γ-coordination environment represents a conformation in which the metal interacts only weakly with the protein (such as via an intervening water molecule), if the metal−nucleotide complex is bound at all. It is possible that at low pH only the nucleotide but not the metal center makes direct contact with the protein.

α-*Conformation.* The conformations of the vanadyl ion with relatively high ligand field strength at neutral pH cannot solely be attributed to either equatorial phosphate oxygen coordination or water coordination nor to a mixture of these but must involve ligands with relatively small $A^{||}_i$ values. Assuming that the complex possesses two equatorial phosphate oxygens, for at least the ATP-bound case, the experimental value for the α-conformation of $A^{||} \approx 152 \times 10^{-4}$ cm^{-1} can only be attained when the other two ligands have a very small value for $A^{||}_i$. This is the case, for example, for two amino acid R−O$^-$ ligands ($A^{||}_i = 141.3 \times$

Scheme 1: Model of the Proposed Equatorial Ligand Composition of the VO^{2+} Ion in the Presence of Nucleotides and the Nitrogenase Fe Protein, Compatible with the Vanadyl Spin Hamiltonian Parameters[a]

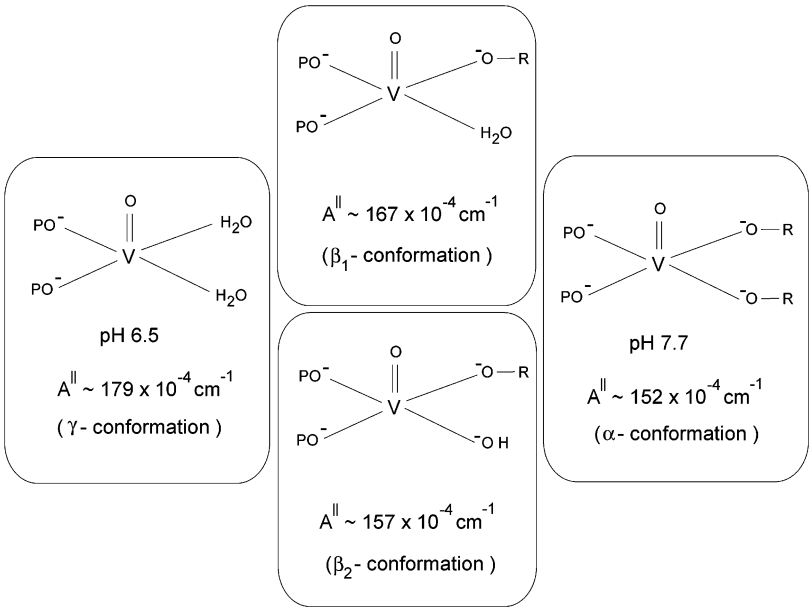

[a] This model is based on the assumption of two equatorially coordinating phosphate groups.

10^{-4} cm^{-1}), such as from serine or threonine side-chain oxygens, yielding $A^{||}_{calc} = 156 \times 10^{-4}$ cm^{-1}. Thus we conclude that the most probable equatorial ligand composition for the α-conformation is that with two phosphate oxygens and two $R-O^-$ ligands from the Fe protein. This assignment is supported by the comparison with the only other VO^{2+}-substituted protein complex, the F_1-ATPase (*21*, *41*). Interestingly, our EPR parameters are compatible with the bidentately coordinated ADP catalytic active site in spinach chloroplast F_1-ATPase (*21*) which has likewise shown a very low $A^{||}$ value of 155.8×10^{-3} cm^{-1}.[6] We can, however, not exclude the possibility that for Kp2 one of the two putative phosphate ligands, in the Fe protein coordination scheme, is occupied by another ligand which possesses an $A^{||}_i$ value close to that of a coordinating phosphate oxygen such as from a coordinating carboxyl side group.

A rhombic distortion of the EPR parameters has been observed for the α-conformation of Kp2. Such a coordination environment might indicate a distortion of the metal symmetry, such as a mixed tridentate nucleotide coordination with equatorial and axial ligands. In fact, for F_1-ATPase, it was argued that such a facial tridentate coordination structure should give rise to a considerable rhombic distortion of the VO^{2+} EPR spectrum (*21*). Intriguingly, one of the F_1-ATPase sites also showed a noticeable rhombicity of the EPR parameters.

β-Conformation(s). The other coordination environments [β-conformation(s)], only observed at more neutral pH, have intermediate experimental $A^{||}$ values and thus represent conformations for which one of the equatorial coordination positions, occupied in the α-conformation by $R-O^-$ ligands, could be occupied by a hydroxyl group or water molecule, yielding values of $A^{||}_{calc} = 159.5 \times 10^{-4}$ cm^{-1} and 166.7×10^{-4} cm^{-1}, respectively. These calculated $A^{||}$ values are close to the experimental values (cf. Table 1) used for the proposed equatorial ligation. The $A^{||}$ values for the β-conformation varied depending on the specific preparation so that it is possible that not only one but two distinct β-conformations coexist, labeled β_1 and β_2. Intriguingly, very similar EPR parameters are observed for all three EPR subspectra in VO-ATP and VO−ADP bound to Kp2; thus it appears that homologous metal coordination environments are present with both nucleotides in all three conformations.

The tentative model for the equatorial vanadyl ligand compositions for the various, inequivalent conformations as a function of pH is illustrated in Scheme 1. The proposed coordination environments for the three conformations suggest that protonation/deprotonation reactions and bond formation with specific equatorial donor groups account for the different spin Hamiltonian parameters. On the basis of this model, a pH-dependent sequence of rearrangements at the metal−nucleotide binding site occurs in the presence of Kp2.

There are several ways that could cause the simultaneous occupancy of distinctly different binding conformations. The different occupancies as a function of pH pertaining to protonation/deprotonation reactions are not unusual (e.g., refs *19* and *42*). Two pH-dependent inequivalent VO^{2+} coordination environments were, for example, found with horse spleen apoferritin (*28*). The metal environments were subsequently studied in more detail by ESEEM (*44*) where these two forms were related to a protonation/deprotonation of one of the cis ligands. On the other hand, the Fe protein possesses two metal−nucleotide binding sites, one on each of the homodimers. Therefore, it is tempting to relate the simultaneous occupancy of two distinctly different binding conformations, that we detect for concentrations <2 VO^{2+}/protein at neutral pH, to the catalytic requirement of nitrogenase for at least

[6] Despite the close homology of the spin Hamiltonian parameters for the γ- and α-conformations of Kp2 with two of the VO^{2+}−nucleotide binding sites in the F_1-ATPase, and hence perhaps their coordination environments, it should be noted that the F_1-ATPase conformations of the VO^{2+}−nucleotide studies have all been carried out for preparations at neutral to high pH.

two hydrolyzable ATP molecules. In fact, two very different MgATP binding sites have been observed in the crystal structure of the [Av1−Av2] complex with an altered Fe protein (*11*). Thus the simultaneous presence of two inequivalent metal−nucleotide conformations, irrespective of the site composition, suggests that the local metal coordination environment might be associated with the formation of two sites which could become independently protonated/deprotonated and hydrated/dehydrated. Yet another interpretation is possible; it is known that two independent ATPase reactions exist for the Fe protein, one of which is related to the catalytic activity of the enzyme while the other is associated with a reduction-independent ATPase cycle (*45*). Thus, it is also possible that the different coordination environments are associated with these two reactions.

For other VO^{2+}−nucleotide complexes, after exchange into D_2O, couplings to a coordinating phosphate group occasionally give rise to a resolvable structure of the parallel EPR lines (*31*, *46*). No such shf structure was observed here. This lack of a resolvable structure is consistent with earlier observations for VO^{2+} in enzymes with coordination to more than one phosphate group such as pyruvate kinase (*47*) and one of the sites in F_1-ATPase (*48*). A coupling to a single phosphate should result in a more easily resolvable doublet of 1:1 intensity ratio while the coupling to two phosphate groups with a 1:2:1 line pattern is often not resolved. This is particularly the case when the couplings are slightly inequivalent. A second site of F_1-ATPase, on the other hand, shows the typical 1:1 pattern characteristic of monodentate coordination (*48*). Thus we suggest that VO^{2+} in the presence of Kp2 is coordinated by more than one, and most probably two, nucleotide phosphate groups at all pH values investigated. This is assumed to be the case for both VO−ATP and VO−ADP since there are no significant differences between the EPR parameters or the line widths of the two nucleotides.

There are striking homologies between the nitrogenase Fe protein and other nucleotide binding proteins (NBP's) in the amino acid sequences (*49*) and, to some extent, in tertiary structures (*8*). The Fe protein contains a characteristic conserved amino acid sequence of the form G·X·X·X·X·K·S/T (where X represents any amino acid residue), known as Walker motif A (*50*) that had been identified as being involved in metal−nucleotide binding in a number of proteins. This motif is usually located close to the carboxyl terminus of the protein between the end of a loop region, called the P-loop, and the start of a α-helix. However, not all NBP's possess a Walker A motif, but those that do are very likely to bind nucleotides. Interestingly, the proposed metal coordination structure for the neutral pH form (α-conformation) with VO−ATP bound is consistent with the X-ray crystal structures of other NBP's having the Walker motif A.[7] These other NBP's are the GTP hydrolases (G-proteins) p21Ras (*37*, *51*−*53*), $G_{i\alpha1}$ (*54*), the elongation factor-Tu (*55*, *56*), transducin-α (*57*), and the ATPase RecA (*58*). All of these NBP's have a common serine or threonine residue of the Walker motif A that directly coordinates the metal corresponding to Ser16 in the Av2 crystal structure (cf. Figure 1) (Ser17 in *K. pneumoniae*). In addition to this residue a second Ser/Thr residue presumably coordinates the metal only in the ATP/GTP-bound state (*52*, *56*, *57*). The Fe protein also appears to contain two other conserved features, based on the proposed homology with small GTPases, the switch I and switch II regions. These are the two regions that presumably undergo the most pronounced conformational rearrangements upon ATP hydrolysis. The equatorial metal coordination of the α-conformation that we deduce is consistent with the structure observed for the proteins above with a second amino acid side-chain oxygen coordinating the metal center in the "on" conformational state. These other proteins exhibit a critical rearrangement in the ATP-bound state especially through a second Thr/Ser ligand in the switch I region (effector loop) moving close enough to directly coordinate the nucleotide-bound metal ion. This structure has not yet been observed for the nucleotide binding sites of the nitrogenase Av2 complex with AlF_4^- (*10*) or in an altered Av2, carrying a deletion at Leu127, when bound to Av1 in the presence of MgATP (*11*). However, in the latter case the mutation alters the Fe protein nucleotide binding site so that the metal−ATP coordination may not be the same as that in the native, wild-type protein. Unfortunately, there are no comparable EPR data available on other GTP and ATPases for vanadyl-substituted proteins.

The X-ray crystal structures of the ADP/GDP-bound state have also been determined for most of the proteins mentioned above. The diphosphate nucleoside structure with VO^{2+}, proposed in the present study, is, however, incompatible with the structures of other NBP's or the Fe protein. The homology of the VO−ADP and VO−ATP bound EPR spectra of Kp2 suggests that one of the critical conformational changes of the metal−nucleotide binding site that regulates protein function might be missing or disturbed when VO^{2+} replaces Mg^{2+}. The X-ray structure of the Fe protein also shows that an aspartic acid (Asp39 for Av2) is bound to the metal via an intervening water molecule. This residue has been mutated with significant effects on the protein properties. The Asp39 → Asn altered Fe protein exhibits substrate inhibition and altered interprotein interactions (*59*). Interestingly, nitrogenase inhibition by the altered protein is remarkably similar to inhibition by vanadyl. This allows us to suggest that VO^{2+} substitution may affect the metal coordination environment in a manner similar to the mutation of the protein without any direct intervention at the protein. In addition, also the Asp129 → Glu altered Fe protein was inactive (*60*). Thus vanadyl substitution may have a similar effect on the signal transduction pathway believed to regulate interprotein interactions as the altered proteins.

However, exceptions also exist to typical nucleotide binding configurations harboring the Walker sequences A and B, such as the Rho superfamily (*61*, *62*). X-ray crystallography has shown GDP binding structures with Mg^{2+} that deviate significantly from those of the above Mg^{2+}−NBP's with the most noticeable differences in the switch I region. Remarkably, they are compatible with the metal environment observed here with VO^{2+}; i.e., they possess only three water molecules bound and two metal-coordinated threonine residues in the GDP-bound case. This contrasts the above ATP/GTPases but maintains the monodentate β-phosphate oxygen coordination with GDP.

[7] It should be noted that the Av2 crystal structures should correspond to the neutral pH form since crystals were presumably grown at pH 8.5 (*9*).

The probable inability to undergo such rearrangement upon hydrolysis could explain nitrogenase inhibition by VO^{2+}. Conversely, the pH dependence of the inner-sphere metal coordination going from the γ- to the α-conformation indicates that the pH modulates one of the essential conformational rearrangements, suggesting that the pH dependence for maximal nitrogenase activity might be coupled to the ability of the Fe protein to undergo one of these critical changes.

There is a debate about sometimes deviating metal coordination structures in G-proteins with a missing or only weakly interacting second ligand (*63*−*65*). The presence of one or possibly two conformations observed in the present study [β-conformation(s) that lack a second equatorial $R-O^-$ ligand in the ATP(GTP)-bound case] may help to resolve this controversy if such a conformation is also adopted by G-proteins in the Mg^{2+}- or Mn^{2+}-bound forms. This behavior might also be capable to explain the differences between the solution and crystalline state or polycrystalline structures (*66*) since small changes of pH may already lead to shifts of the occupancy of the conformations.

It remains to be mentioned that, without knowing the identities of at least some of the equatorial ligands reasonably firmly, the identification of the others, purely on the basis of the EPR parameters, must remain somewhat speculative. Other, higher resolution, spectroscopic techniques such as ENDOR or ESEEM need to be employed in order to further confirm the assignments.

In summary, changes in the coordination environment of VO^{2+}-substituted nucleotides in the presence of Kp2 have been detected by EPR. These depend on pH, the specific nucleotide, and the oxidation level of the [4Fe-4S] center in the protein. Thus the coordination structure of the metal bound to the nucleotide and concomitantly the associated control of the nitrogenase Fe protein function is much more complex than previously assumed.

ACKNOWLEDGMENT

EPR simulations of the VO^{2+} spectra were carried out using the program LSIM written by Dr. D. Collison and kindly provided by Dr. S. Fairhurst. We thank Dr. S. M. Roe for assistance in comparing the Av2 and p21Ras X-ray crystal structures.

REFERENCES

1. Eady, R. R. (1986) in *Nitrogen Fixation, Vol. 4: Molecular Biology* (Broughton, W. J., and Pühler, S., Eds.) pp 1−49, Clarendon Press, Oxford.
2. Mortenson, L. E., Seefeldt, L. C., Morgan, T. V., and Bolin, J. T. (1993) in *Advances in Enzymology* (Meister, A., Ed.) Vol. 67, pp 299−374, Wiley & Sons, New York.
3. Burgess, B. K., and Lowe, D. J. (1996) *Chem. Rev. 96*, 2983−3011.
4. Tso, M. Y. W., and Burris, R. H. (1973) *Biochim. Biophys. Acta 309*, 263−270.
5. Stephens, P. J., McKenna, C. E., Smith, B. E., Nguyen, H. T., McKenna, M. C., Thomson, A. J., Devlin, F., and Jones, J. B. (1979) *Proc. Natl. Acad. Sci. U.S.A. 76*, 2585−2589.
6. Ashby, G. A., and Thorneley, R. N. F. (1987) *Biochem. J. 246*, 455−465.
7. Schlessman, J. L., Woo, D., Joshua-Tor, L., Howard, J. B., and Rees, D. C. (1998) *J. Mol. Biol. 280*, 669−685.
8. Georgiadis, M. M., Komiya, H., Chakrabarti, P., Woo, D., Kornuc, J. J., and Rees, D. C. (1992) *Science 257*, 1653−1659.
9. Jang, S. B., Seefeldt, L. C., and Peters, J. W. (2000) *Biochemistry 39*, 14745−14752.
10. Schindelin, H., Kisker, C., Schlessman, J. L., Howard, J. B., and Rees, D. C. (1997) *Nature 387*, 370−376.
11. Chiu, H.-J., Peters, J. W., Lanzilotta, W. N., Ryle, M. J., Seefeldt, L. C., Howard, J. B., and Rees, D. C. (2001) *Biochemistry 40*, 641−650.
12. Orme-Johnson, W. H., Hamilton, W. D., Ljones, T., Tso, M. Y. W., Burris, R. H. Shah, V. K., and Brill, W. J. (1972) *Proc. Natl. Acad. Sci. U.S.A. 69*, 3142−3145.
13. Smith, B. E., Lowe, D. J., and Bray, R. C. (1973) *Biochem. J. 135*, 331−341.
14. Rees, D. C., and Howard, J. B. (1999) *J. Mol. Biol. 293*, 343−350.
15. Ballhausen, C. J., and Gray, H. B. (1962) *Inorg. Chem. 1*, 111−122.
16. Lanzilotta, W. N., Parker, V. N., and Seefeldt, L. C. (1998) *Biochemistry 37*, 399−407.
17. Thorneley, R. N. F., and Lowe, D. J. (1983) *Biochem. J. 215*, 393−403.
18. Slebodnik, C., Hamstra, B. J., and Pecoraro, V. L. (1997) *Struct. Bonding 89*, 51−106.
19. Chasteen, N. D. (1981) *Biol. Magn. Reson.3*, 53−119.
20. Petersen, J., Hawkes, T. R., and Lowe, D. J. (1997) *J. Biol. Inorg. Chem. 2*, 308−319.
21. Houseman, A. L. P., LoBrutto, R., and Frasch, W. D. (1995) *Biochemistry 34*, 3277−3285.
22. Stankiewicz, P. J., Tracey, A. S., and Crans, D. C. (1995) *Met. Ions Biol. Syst. 31*, 287−324.
23. Lindquist, R. N., Lynn, J. L., and Lienhard, G. E. (1973) *J. Am. Chem. Soc. 95*, 8762.
24. Elberg, G., Li., J., and Shechter, Y. (1994) *J. Biol. Chem. 269*, 9521−9527.
25. Albanese, N. F., and Chasteen, N. D. (1978) *J. Phys. Chem. 82*, 910−914.
26. Cini, R., Giorgi, G., Laschi, F., Sabat, M., Sabatini, A., and Vacca, A. (1989) *J. Chem. Soc., Dalton Trans.*, 575−580.
27. deKoch, R. J., West, D. J., Cannon, J. C., and Chasteen, N. D. (1974) *Biochemistry 21*, 4347−4354.
28. Chasteen, N. D., and Theil (1982) *J. Biol. Chem. 257*, 7672−7677.
29. deBoer, E., Boon., K., and Wever, R. (1988) *Biochemistry 27*, 1629−1635.
30. Bogumil, R., Hüttermann, J., Kappl, R., Stabler, R., Sudfeldt, C., and Witzel, H. (1991) *Eur. J. Biochem. 196*, 305−312.
31. Mustafi, D., Telser, J., and Makinen, M. W. (1992) *J. Am. Chem. Soc. 114*, 6219−6226.
32. Parker, C. C., Reeder, R. R., Richards, L. B., and Rieger, P. H. (1970) *J. Am. Chem. Soc. 92*, 5230−5231.
33. Cini, R., Burla, M. C., Nunzi, A., Palidori, G. P., and Zanazzi, P. F. (1984) *J. Chem. Soc., Dalton Trans.*, 2467−2476.
34. Petersen, J., Fisher, K., and Lowe, D. J. (2002) to be submitted for publication.
35. Petersen, J., Mitchell, C. J., Fisher, K., and Lowe, D. J. (2002) to be submitted for publication.
36. Smithers, G. W., Poe, M., Latwesen, D. G., and Reed, G. H. (1990) *Arch. Biochem. Biophys. 280*, 416−420.
37. Latwesen, D. G., Poe, M., Leigh, J. S., and Reed, G. H. (1992) *Biochemistry 31*, 4946−4950.
38. Cornman, C. R., Geiser-Bush, K. M., Rowley, S. P., and Boyle, P. D. (1997) *Inorg. Chem. 36*, 6401−6408.
39. Carl, P. J., Isley, S. L., and Larsen, S. C. (2001) *J. Phys. Chem. A 105*, 4563−4573.
40. Smith, T. S., II, Root, C. A., Kampf, J. W., Rasmussen, P. G., and Pecoraro, V. L. (2000) *J. Am. Chem. Soc. 122*, 767−775.
41. Buy, C., Matsui, T., Andrianambinintsoa, S., Sigalat., C., Girault, G., and Zimmermann, J.-L. (1996) *Biochemistry 35*, 14281−14293.
42. Rehder, D. (1995) *Met. Ions Biol. Syst. 31*, 1−44.
43. Rees, D. C., Chan, M. K., and Kim, J. (1993) *Adv. Inorg. Chem. 40*, 89−119.
44. Gerfen, G. J., Hanna, P. M., Chasteen, N. D., and Singel, D. J. (1991) *J. Am. Chem. Soc. 113*, 9513−9519.
45. Thorneley, R. N. F. (1992) *Philos. Trans. R. Soc. London, Ser. B 336*, 73−82.
46. Markham, G. D., and Leyh, T. S. (1987) *J. Am. Chem. Soc. 109*, 599−600.
47. Lord, K. A., and Reed, G. H. (1990) *Arch. Biochem. Biophys. 281*, 124−131.

48. Houseman, A. L. P., LoBrutto, R., and Frasch, W. D. (1994) *Biochemistry 33*, 10000−10006.
49. Robson, R. L. (1984) *FEBS Lett. 173*, 394−398.
50. Walker, J. E., Saraste, M., Runswick, M. J., and Gay, N. J. (1982) *EMBO J. 1*, 945−981.
51. Pai, E. F., Kabsch, W., Krengel, U., Holmes, K. C., John, J., and Wittinghofer, A. (1989) *Nature 341*, 209−214.
52. Pai, E. F., Krengel, U., Petsko, G. A., Goody, R. S., Kabsch, W., and Wittinghofer, A. (1990) *EMBO J. 9*, 2351−2359.
53. Milburn, M. V., Tong, L., deVos, A. M., Brünger, A., Yamaizumi, Z., Nishimura, S., and Kim, S.-H. (1990) *Science 247*, 939−945.
54. Coleman, D. E., Berghuis, A. M., Lee, E., Linder, M. E., Gilman, A. G., and Sprang, S. R. (1994) *Science 265*, 1405−1411.
55. Kjeldgaard, M., Nissen, P., Thirup, S., and Nyborg, J. (1993) *Structure 1*, 35−50.
56. Berchtold, H., Reshetnikova, L., Reiser, C. O. A., Schirmer, N. K., Sprinzl, M., and Hilgenfeld, R. (1993) *Nature 365*, 126−132.
57. Noel, J. P., Hamm, H. E., and Sigler, P. B. (1993) *Nature 366*, 654−663.
58. Story, R. M., and Steitz, T. A. (1992) *Nature 355*, 374−376.
59. Lanzilotta, W. N., Fisher, K., and Seefeldt, L. C. (1997) *J. Biol. Chem. 272*, 4157−4165.
60. Lanzilotta, W. N., Ryle, M. J., and Seefeldt, L. C. (1995) *Biochemistry 34*, 10713−10723.
61. Wei, Y., Zhang, Y., Derewenda, U., Liu, X., Minor, W., Nakamoto, R. K., Somlyo, A. V., Somlyo, A. P., and Derewenda, Z. S. (1997) *Nat. Struct. Biol. 4*, 699−703.
62. Hoffman, G. R., Nassar, N., and Cerione, R. A. (2000) *Cell 100*, 345−356.
63. Halkides, C. J., Farrar, C. T., Larson, R. G., Redfield, A. G., and Singel, D. J. (1994) *Biochemistry 33*, 4019−4035.
64. Bellew, B. F., Halkides, C. J., Gerfen, G. J., Griffin, R. G., and Singel, D. J. (1996) *Biochemistry 35*, 12186−12193.
65. Halkides, C. J., Bellew, B. F., Gerfen, G. J., Farrar, C. T., Carter, P. H., Ruo, B., Evans, D. A., Griffin, R. G., and Singel, D. J. (1996) *Biochemistry 35*, 12194−12200.
66. Rohrer, M., Prisner, T. F., Brügmann, O., Käss, H., Spoerner, M., Wittinghofer, A., and Kalbitzer, H. R. (2001) *Biochemistry 40*, 1884−1889.

BI0260029